Fibrillation of Egg White Ovalbumin: A Pathway via Biomineralization

ARTICLE *in* THE JOURNAL OF PHYSICAL CHEMISTRY B · MARCH 2011

Impact Factor: 3.3 · DOI: 10.1021/jp200607x · Source: PubMed

THE JOURNAL OF PHYSICAL CHEMISTRY B

ARTICLE

pubs.acs.org/JPCB

Fibrillation of Egg White Ovalbumin: A Pathway via Biomineralization

Prabir Pal,[†] Mrityunjoy Mahato,[†] Tapanendu Kamilya,[‡] Bidisha Tah,[†] Ratan Sarkar,[§] and G. B. Talapatra*[,†]

[†]Department of Spectroscopy, Indian Association for the Cultivation of Science, Jadavpur, Kolkata-700 032, India

Supporting Information

ABSTRACT: Here we report the fibrillation of egg white ovalbumin (OVA) induced by the biomineralization of two alkali halides (KCl, NaCl) in the Langmuir−Blodgett (LB) film of OVA. The pressure−area isotherm of OVA shows the salt-induced increment of apparent area/monomer of OVA. Fibrillation of OVA in the LB film is monitored by FE-SEM imaging. Formation of fibrillar aggregates is concomitant with an increase of salt concentration. HR-TEM and EDX measurements allowed us to identify nanostructured crystals of salt, which are associated with this fibrillar structure. FTIR spectroscopic study of the amide band in LB films as well as CD spectroscopy in solution qualitatively indicates the increase in β-sheet to α-helix ratio in the presence of salt, indicating unfolding of protein. We suggest that the ion attachment to the peptide chain leads to unfolding and that subsequent recrystallization in the transferred monolayer leads to fibrillation of protein as well as biomineralization of alkali halide salts. This finding demonstrates that the fibrillation of OVA is induced by the biomineralization of alkali halides.

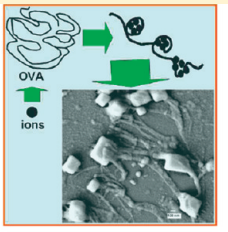

Salt induced Protein fibrillation

1. INTRODUCTION

Fibrillation of proteins and peptides is a kind of directional self-aggregation process, leading to the formation of oligomers under specific biophysiochemical conditions/environments.[1−3] This basic process is associated with the amyloid fibril formation in Alzheimer's disease, Parkinson's disease, etc.[1,4] Materials science, biomedical science, and tissue and scaffold engineering have placed enormous scientific demands for the fabrication of fibrous material.[5,6] Therefore, identifying the biophysiochemical factors that can trigger and mediate the fibrillation of proteins is a challenging issue in modern biorelated research. Although many researchers have been devoted to understanding the fibrillation mechanism, very little is known so far regarding the pathway and the mechanism of the fibrillation process. Research have revealed that the fibrillation process is mediated via two steps: first, a critical nucleation center is formed as a starting point, and second, protein aggregation proceeds to form fibril structure.[7] The ability to from fibrils is a generic property of the polypeptide chain, i.e., many proteins are potentially able to form amyloid fibrils under appropriate conditions. In addition, the pH, ionic strength, temperature, denaturing agent, solution hydrophobicity, etc., have some role in some kind of protein misfolding for further aggregation processes.[3,8] Protein misfolding is a stochastic event, which leads to the fibrillation of protein via the interaction between unfolded proteins when it passes through the global minima in free energy landscape.[9] Recent research also revealed that the coordination of metal ions with amyloid fibrils modulates the fibrillation pathway and induces aggregation of proteins.[3,10] In this regard, Pandey et al. showed the enhancement of fibrillation of human serum albumin (HSA) induced by Cu(II) ions utilizing the unfolded state of HSA above 65 °C.[3] The role of protein−nanoparticle corona in the fibrillation of protein is to be noted in this context.[11]

In this article, we report the role of biomineralization as a pathway for the fibrillation of proteins, taking ovalbumin (OVA) as a model protein. OVA is major egg white, surface-active globular protein composed of 385 amino acids with a molecular weight of 45 kDa, and it has been widely studied in our laboratory.[12−16] Here the biomineralization of two alkali halides (KCl and NaCl) was studied in the Langmuir−Blodgett (LB) film of OVA. It has been reported in literature that the biomineralization utilizes organic templates for the nucleation and growth of minerals into crystalline superstructure.[17−19] Recently, Pipich et al. have found that proteins become unfolded by the presence of mineral and form a nucleation center to proceed the biomineralized superstructure.[20] This necessarily indicates that the biomineralization has some effect on the protein structure during the mineralization process.[20,21]

Here, interestingly, the fibrillation of OVA is observed in an attempt to study the biomineralization of KCl and NaCl. However, we have not adopted any protocol for the initial destabilization in helical structure of OVA, though the surface tension at the air/water interface has a small contribution in the unfolding of protein, yet it is not as effective as pH, temperature, etc.[22] Pearce et al. reported the temperature-induced fibrillation of OVA.[23] OVA has shown its potential in the biomineralization of hydroxypatite[24] and calcium carbonate ($CaCO_3$).[20,25]

Here we have adopted the LB technique to build up monolayers of OVA and to transfer it onto substrate as well as to monitor the biomineralization of KCl and NaCl. Fourier transform infrared (FTIR) spectroscopy and circular dichroism (CD) spectroscopy were employed to characterize the OVA and

Received: January 20, 2011
Revised: March 7, 2011
Published: March 23, 2011

OVA−fiber at the secondary structure level. The high-resolution transmission electron microscope (HR-TEM), energy-dispersive X-ray spectroscopy (EDX), and field emission scanning electron microscopy (FE-SEM) were used to characterize the inorganic crystals (KCl/NaCl) and organic−inorganic hybrid part. By these combined studies, efforts were made to understand biomineralization as a pathway to induce the fibrillation of OVA.

2. EXPERIMENTAL SECTION

2.1. Materials. OVA was purchased from Sigma (St. Louis, MO). NaCl and KCl were purchased from Merck Chemical Co. and used as received without further purification.

2.2. Methods. *2.2.1. Surface Pressure−Area (π−A) Isotherm Measurement.* The surface pressure−area (π−A) isotherms measurements were performed in a computerized LB trough (model 2000C, Apex Instruments Co., India) in pure water and salt-containing water subphases. A known amount of aqueous solution of OVA with a concentration (C_{OVA}) of 0.1 mg/mL was spread on the air/water interface for isotherm measurements. The other protocols used were well illustrated in our earlier reports.[12,13] Milli-Q water with pH = 5.5 and resistivity = 18.2 MΩ-cm was prepared using Milli-Q apparatus. This water was used to prepare the subphase and the protein solution. All experiments were performed at temperature 25 ± 0.5 °C, unless otherwise mentioned. At least three independent runs were performed to check the reproducibility.

2.2.2. Monolayer Transfer. The glass (for FESEM) and silicon wafer (for FTIR) substrates were used and cleaned very carefully by the process described in our earlier reports.[12,13] The monolayers were then transferred very carefully at the desired surface pressure with a speed of 5 mm/min onto the appropriate substrate, which was previously immersed in the pure and salted subphases.

2.2.3. Study of Surface Morphology. High-resolution field emission scanning electron microscopy (FE-SEM, model no. JEOL JSM-6700 F), with a range of 0.5−30 kV and lateral resolution of 1.2−2.2 nm, was employed to extract the surface morphology of all transferred LB films on a fine hydrophilic glass substrate. The LB films were platinum (Pt) coated to enable conduction for imaging by Pt sputtering.

The high-resolution transmission electron microscopy (HR-TEM, model JEOL-JEM-2011), with an operating voltage of 200 kV, was used for high-resolution imaging and material characterization. A 300-mesh carbon-coated copper grid was used as a substrate. Dispersive X-ray spectroscopy (EDX) was also performed with TEM model JEOL-JEM-2011.

2.2.4. FTIR and CD Spectroscopy. FTIR spectra of OVA−LB films, lifted at 20 mN/m from pure water and KCl-containing subphases, on silicon wafers were recorded at room temperature with a Magna-IR (model no. 750 spectrometer, series II, Nicolet, Madison, WI). In all the cases, the data were averaged over 100 scans. The resolution of the instrument was 4 cm^{-1}. The deconvolution of the amide-I FTIR band was performed by Gaussian multipeak fitting to determine the different conformations of OVA at various conditions. The details of this protocol were described in our earlier reports.[26,27]

CD spectra of OVA (0.05 g/L) in pure water and in aqueous KCl solution were recorded at room temperature on a JASCO J-815 CD spectrometer (model no. J-815-150 S) with 10 mm path length. Three scans were adapted to decrease the noise of the CD spectra. The secondary structures of pure OVA (such as α-helix, β-sheet, turn, unordered, etc.) were calculated from the CD data using the SELCON3 (CD-Pro) program, choosing a reference set of 43 proteins.[28]

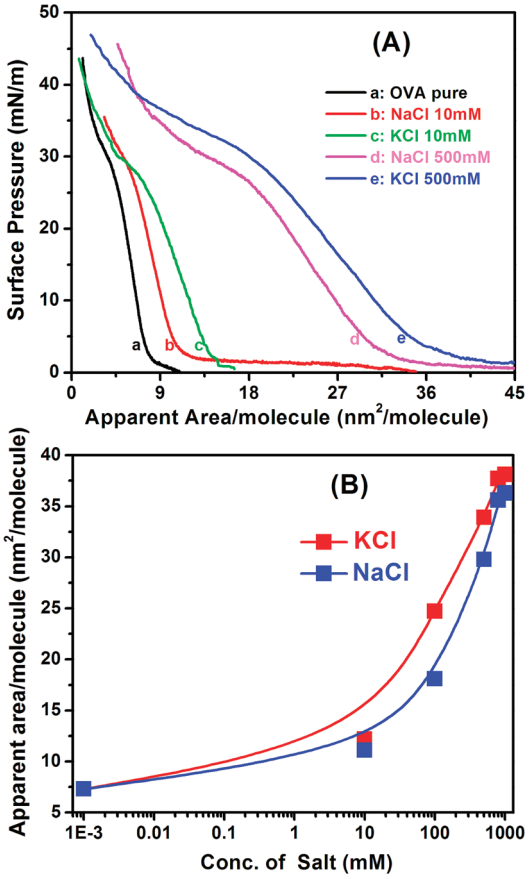

Figure 1. (A) π−A isotherm of OVA with different concentrations of KCl and NaCl in the subphase. (B) Plot of area/molecule (measured at 5 mN/m) of OVA with varying salt (KCl, NaCl) concentrations.

3. RESULTS AND DISCUSSION

3.1. Salt−OVA Interaction in the Langmuir Monolayer by π−A Isotherm Study. We have measured the pressure−area (π−A) isotherm of OVA (Figure 1A) after spreading a measured amount of OVA solution at the air/water interface. The subphase was either pure water or salt water having different concentrations of KCl/NaCl. OVA is soluble in water, but because of its amphiphilicity it has a tendency to be retained at the air/water interface through structural reorganization. The amount of surface coverage varies from protein to protein as well as from the ion concentration in the subphase. It is evident from Figure 1A that OVA is a surface-active protein, forming a Gibbs/Langmuir monolayer at the air/water interface. Moreover, in the presence of KCl/NaCl, the surface activity changes, reflected by the increase in apparent area/molecule (Figure 1B).

The changes in apparent area/molecule were measured at the gaseous to liquid (G−L) transition region, at a 5 mN/m pressure of the Langmuir monolayer of OVA at different subphases.[12] This change in apparent area/molecule necessarily represents the ion−protein interaction that follows the well-known DLVO (Derjaguin, Landau, Verwey, and Overbeek) theory, which is more elaborately described in our earlier reports.[29,30] According

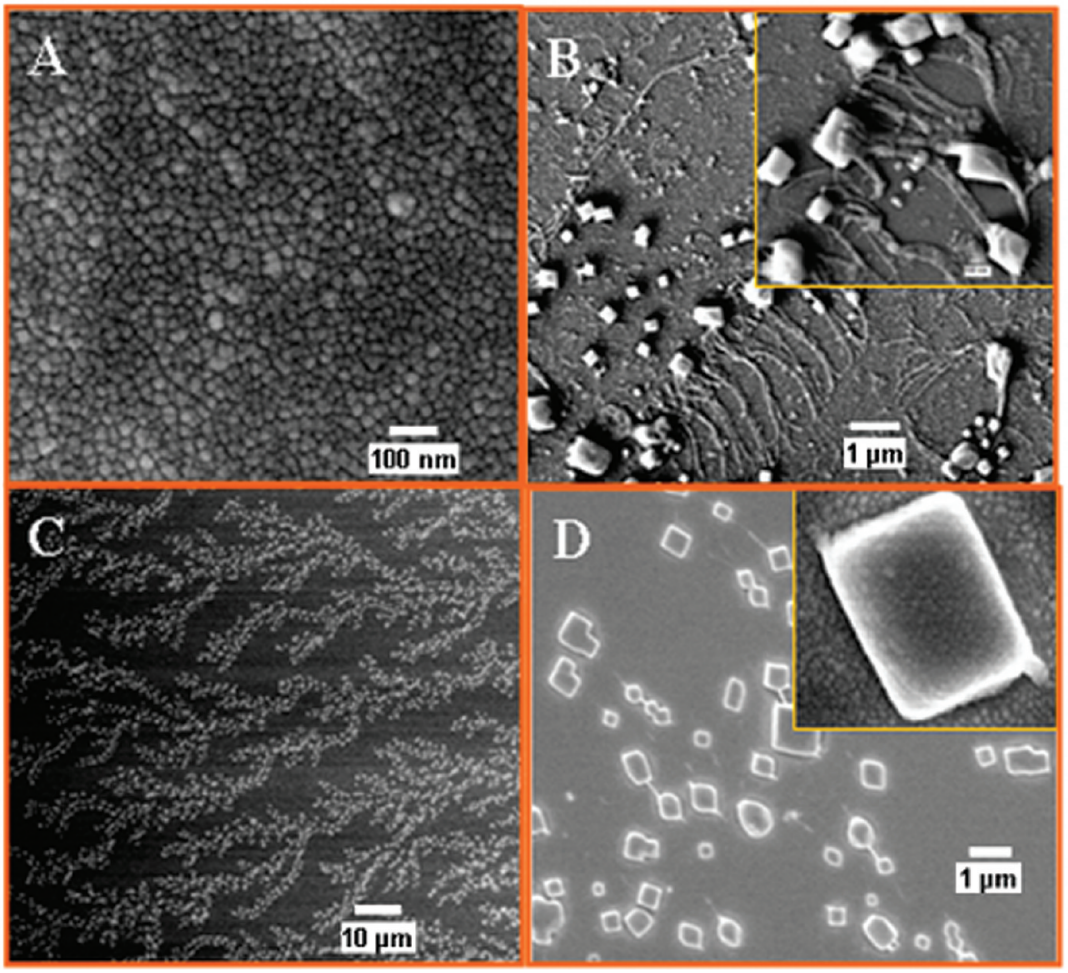

Figure 2. FE-SEM images of (A) OVA pure LB film and (B) OVA−NaCl LB film during the biomineralization, showing the fibril structure of OVA. The inset in panel B shows the magnified OVA fiber. (C) OVA−KCl LB film showing the fractal structure of the OVA−KCl crystal. (D) OVA−KCl fiber and crystal at higher magnification. The inset shows the magnified single KCl crystal with a diagonal fiber tip.

to DLVO theory, this ion−protein interaction is attributed to repulsive electrostatic and attractive Van der Waal forces, which may certainly contribute to the biomineralization of alkali halides (KCl/NaCl) at the amino acid residues of proteins (OVA) as well as in the unfolding of OVA.[17,20]

3.2. FE-SEM Study. We have lifted the LB monolayer of OVA on a hydrophilic glass substrate from pure water and from salt (NaCl/KCl)-containing subphase at the condensed region (35 mN/m). The salt concentration was maintained at 0.5 M in the subphase. Stabilization time was 1 h. Figure 2 shows the FE-SEM images of LB films of OVA lifted from pure water subphase as well as from salted subphase. Figure 2A shows that the LB film of pure OVA comprises a globular unit of OVA with a diameter of ∼20−30 nm, which is much larger than the monomeric size (∼7 nm) of OVA as assigned from the crystallographic structure of OVA (7 nm × 4.5 nm × 5 nm).[12,31] On the other hand, FE-SEM images (Figure 2B) of the LB films of OVA in subphase containing NaCl show that the biomineralization of NaCl has taken place along the OVA fibers. The fiber consists of interconnected globular protein aggregates. It is well-known that proteins may exist in multimeric form for tertiary structure in aqueous solution depending on the conditions of the aqueous solution. In this case, the multimeric structure appears due to the high electrolyte concentration present in the solution, which shields the electrostatic repulsion between protein monomers and favors attractive interaction. Therefore, the globular unit actually represents aggregates of several monomers. Figure 2C and 2D shows the fractal structure of OVA−biomineralized KCl crystal at different magnifications. More interestingly, the OVA fibers are formed at the junction between biomineralized KCl crystals. Here the biomineralized crystals were characterized by HR-TEM, EDX, and the JCPDS data bank; furthermore, the OVA fibers were characterized by CD and FTIR spectroscopy as discussed later. Here the biomineralization facilitates the fibrillation of OVA, and our FE-SEM data corroborate our results discussed previously.[20] Here the biomineralization of KCl promotes the unfolding and aggregation of OVA in a fibrillar fashion (Figure 2C and 2D).[20,32] Moreover, the OVA fibers also facilitate the biomineralization of KCl via ion−protein interaction, leading to alignment of the crystals in a particular fashion (such as network, fractal, etc.).[20,33] Note that the evaporation factor may have a small contribution to the assembly of the crystal in the protein matrix. The fractal-like structure (mean fractal dimension is 1.414 calculated by the box count method using the ImageJ program) of the biomineralized KCl crystal and alignments are probably mediated by the OVA fiber along its fibril direction.[20] In

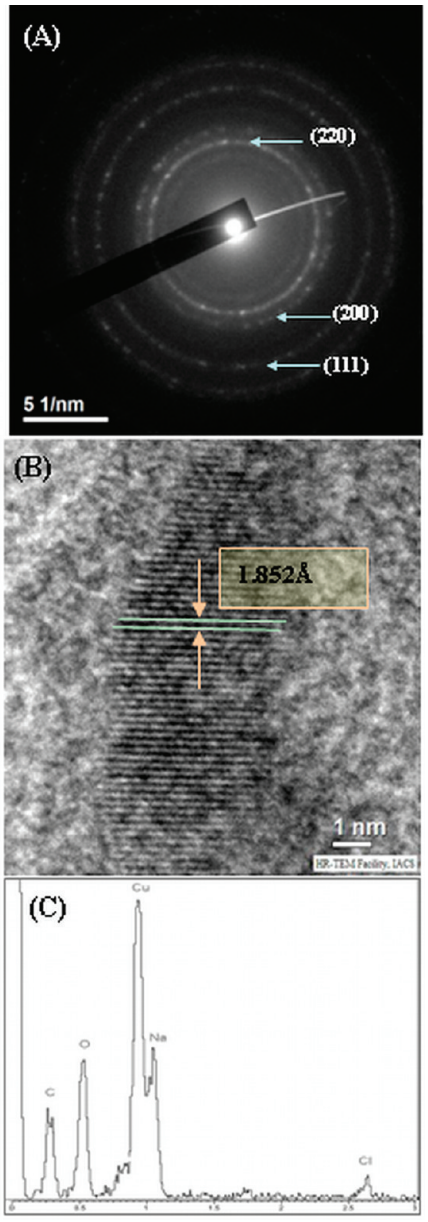

Figure 3. Transmission electron microscopy (TEM) data for the biomineralized NaCl crystal. (A) Selected area electron diffraction (SAED) pattern. (B) The fringe pattern of the NaCl crystal. (C) Energy dispersive X-ray (EDX) spectra of biomineralized NaCl crystal.

this regard, the studies of Iijima et al. and Zhang et al. have shown the orientation of calcium phosphate crystals (*c*-axis) along the collagen fiber template.[34,35]

The thickness of a single fiber ranges from a few nanometers to as large as 100 nm. Note that both the NaCl and KCl crystals are diagonally linked with the fibers, following a kind of array along the fibril direction. Figure 2D shows that the OVA fiber connects both diagonal ends of the crystal. This may indicate that the OVA fiber itself acts as a directional element for the alignment of the crystal. Also note that aligned fractal structures are observed for the KCl crystals but not for NaCl crystals, although in both cases the crystals are associated with the fibers. Moreover, the FE-SEM images show that the fibrillation in OVA−NaCl is much more than that in OVA−KCl. We have found that the salt concentration in the subphase, surface pressure, waiting time, lifting rate, etc., have great influences on fractal structure formation. Thus, some variation in experimental conditions may be one of the causes for the observations of alignment in fractal structures for KCl crystals but not for NaCl crystals. Differences in crystallographic parameters between KCl and NaCl may also contribute toward the specific alignment. A detailed study on fractal structure formation is in progress and will be communicated later. Our results thus show the experimental evidence of protein-mediated mineral nucleation/biomineralization. We suggest that the ion attachment to the peptide chain leads to the unfolding of protein and that subsequent recrystallization in the transferred monolayer leads to the fibrillation of protein. Moreover, the biomineralization of alkali halides further facilitates the unfolding and fibrillation of OVA. This biomineralization of alkali halides (KCl, NaCl) and subsequent fibrillation of OVA is in line with the earlier prediction by Pipich et al. regarding biomineralization of $CaCO_3$ mediated by unfolding of OVA by Ca^{2+} as observed through neutron scattering experiments.[20]

3.3. HR-TEM Study. Figure 3A shows the selected area electron diffraction (SAED) pattern of biomineralized NaCl crystal in LB film lifted from the carbon-coated TEM grid. Figure 3B shows the HR-TEM image with distinct lattice fringes of the NaCl crystal. The SAED pattern, HR-TEM image, and EDX spectra of the biomineralized KCl crystals are presented in the Supporting Information. The SAED pattern of the NaCl crystal having a (220), (200), (111) diffraction ring is in line with the interplanar spacing of 0.193, 0.273, and 0.315 nm of the bulk cubic NaCl crystal (JCPDS 83-1728). The SAED pattern of the KCl crystal having a (222), (220), (200), (111) diffraction ring is in line with the interplanar spacing of 0.181, 0.222, 0.314, and 0.363 nm of the bulk cubic KCl crystal (JCPDS 75-0296) and also with earlier literature.[36]

The interplanar spacing (*d*-values) from the SAED pattern, fringe pattern, as well as JCPDS data for both KCl and NaCl crystals are presented in Table 1. However, the *d*-values from the HR-TEM image for the KCl crystal (0.272 nm) and for the NaCl crystal (0.185 nm) do not correspond to the preferred *d*-values, possibly because the preferred orientation (200) may differ with the diffraction condition. Moreover, the EDX spectra of the crystal show the clear presence of the NaCl (Figure 3A) and KCl (Figure S1) crystal under an organic (C, O) environment. The percentages of the mismatch in *d*-values with respect to the JCPDS data are calculated (Table 1) and found to be small to moderate in a few cases. These mismatches may be due to the presence of protein residues at the biomineralized crystal facet, causing a small lattice mismatch within the crystal, which is analogous to the observation of Xue et al. in the case of a gold nanoplate in the Langmuir monolayer of bovine serum albumin (BSA).[37] In this regard, also note that the artifacts in the JCPDS data obtained using X-ray diffraction are certainly less than that of the Fourier transform HR-TEM data (fringe pattern). This fact may be one of the reasons for the mismatch in *d*-values in Table 1. However, the observed variation may indicate the perturbation due to the presence of protein molecules attached to the crystal.

3.4. FTIR Study. Recently, the FTIR spectroscopy has been found to be an extremely useful tool to characterize proteins, especially in the amide region, and to determine conformational change, denaturation, unfolding, and aggregation.[26,38] Figure 4A and 4B represents the normalized, deconvoluted FTIR spectra in the amide-I band (~1600−1700 cm^{-1}) for LB films of pure OVA and OVA−KCl on silicon wafers, respectively. The amide-I

Table 1. Crystallographic Data of Biomineralized OVA−KCl and OVA−NaCl Crystals As Obtained from HR-TEM and JCPDS Data Bank

biomineralized crystal	2θ (deg)/(hkl)	$d_{\text{SAED pattern}}$ (Å)	$d_{\text{fringe pattern}}$ (Å)	d_{JCPDS} (Å)	mismatch in d value (%)
KCl	50.0/(222)	1.967	2.723	1.810	−8.674
	40.1/(220)	2.247	2.723	2.220	−1.216
	28.2/(200)	3.193	2.723	3.140	−1.688
	24.1/(111)	3.757	2.723	3.632	−3.442
NaCl	47.1/(220)	1.949	1.852	1.928	−1.089
	32.8/(200)	2.266	1.852	2.730	16.996
	28.3/(111)	3.197	1.852	3.148	−1.556

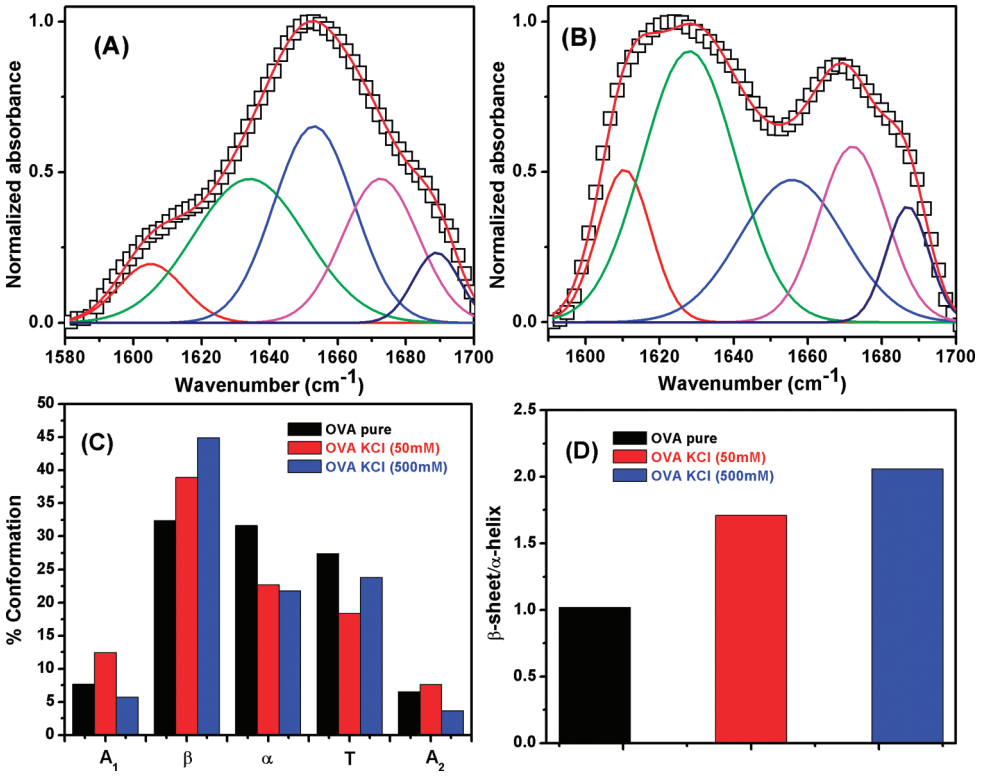

Figure 4. (A, B) Normalized, deconvoluted FTIR amide-I band of OVA and OVA−KCl (0.5 M), respectively. (C) Bar diagram of different conformations of OVA at various concentrations of KCl. (D) Plot of β-sheet over α-helix of pure OVA and OVA−KCl.

band, after deconvolution, represents the contribution of different conformations of protein (such as α-helix, β-sheet, random coil, intra- and intermolecular aggregation, etc.).[27,30]

Here the deconvolution was performed by Gaussian multipeak fitting, and its details were described in our earlier reports.[26,27,30] The amount of α-helix in pure OVA is ∼32.0%, which is in quite good agreement with the earlier data for OVA.[39] There is a change in the conformational elements (α-helix, β-sheet, etc.) of OVA in the biomineralized KCl crystal (Figure 4C). Moreover, the amount of β-sheet in comparison with the α-helix is larger in case the OVA−KCl system. The β/α-ratio progressively increases with the salt concentration (Figure 4D). This increment of β-sheet over α-helix necessarily indicates unfolding as well as aggregation of OVA and probably the formation of a fibril-like structure of OVA.

3.5. CD Spectroscopic Study. We have also measured CD spectra of OVA in pure aqueous and metal halide aqueous solution, which are shown in Figure 5. In the presence of KCl and NaCl, there is a change in the CD spectral signature of OVA. Here the conformational change of OVA is estimated by fitting the CD data using the CD-Pro (SELCON3) program, and it is represented in Table 2. Although a qualitative decrement of molar ellipticity in the 190 nm region at high salt concentration (0.5 M KCl) is observed, the spectrum becomes too noisy and gives erroneous results in the fitting. Table 2 shows that at a lower concentration of salt (10 mM), the decrement of the α-helix and increment of the β-sheet in the presence of alkali halide (KCl, NaCl) necessarily indicates the unfolding of protein and the ion−protein interaction that promotes further biomineralization. Furthermore, the CD data could not confirm the fibril type of aggregation, because there is no apparent presence of a minimum at 215 nm, which is a direct confirmation of the type of β-sheet conformation. Still the increment of β-sheet content in ion−protein solution is merely an indication of aggregation of OVA. Thus, fibrillation of OVA seems to be favored in some way by drying effects, which affects the balance of interactions

dx.doi.org/10.1021/jp200607x |J. Phys. Chem. B 2011, 115, 4259–4265

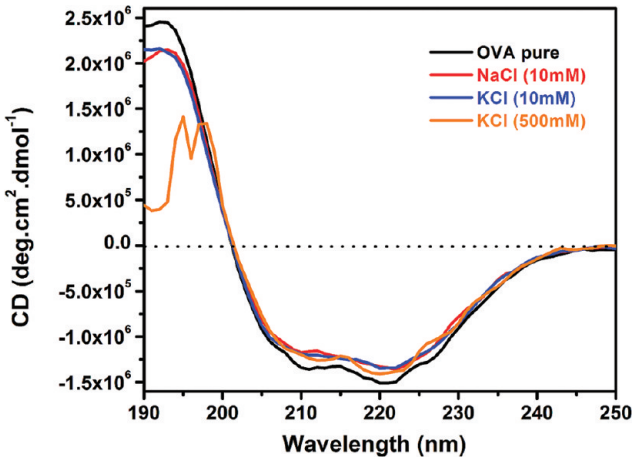

Figure 5. CD spectra of OVA (C_{OVA} = 0.05 g/L) in pure water, in KCl solution, and in NaCl solution, respectively.

Table 2. Secondary Structural Conformation of OVA at Different Conditions from the Fitting of CD Data Using the CD-Pro (SELCON3) Program [a]

sample	α	β	T	U
pure OVA	40.54	15.16	17.40	26.90
OVA−KCl (10 mM)	34.65	16.25	19.60	29.50
OVA−NaCl (10 mM)	35.80	16.50	19.20	28.50

[a] α, β, T, and U represent the α-helix, β-sheet, turn, and unordered conformational elements in the secondary structure of the protein, respectively.

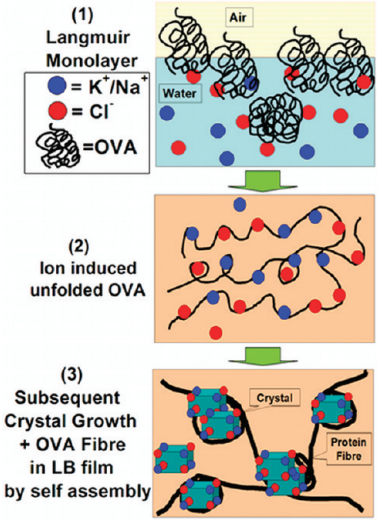

Figure 6. Cartoon of biomineralization (KCl, NaCl)-induced fibrillation of OVA protein in the Langmuir monolayer and transferred LB film.

between protein molecules and ion−protein molecules. There are moderate differences in different conformer percentages in aqueous solution (studied by CD) and in thin film (studied by FTIR), which may be due to the presence or absence of aqueous medium in the two different environments.[30,40] However, as mentioned earlier, here the air/water interface (i.e., in Langmuir film) and the process of transfer to solid support (i.e., in LB film) play some role in the unfolding of OVA, and this may contribute to the differences in the FTIR results in LB film and the CD results in solution.

3.6. Pictorial Description of Biomineralization-Induced Fibrillation. The cartoon presented in Figure 6 describes the fibrillation of OVA induced by biomineralization. The ions (K^+/Na^+, Cl^-) present in the subphase of the LB trough interact and attach with the charged residues of OVA molecules and thus form a Langmuir monolayer with partially unfolded OVA. Subsequently, in the transferred LB film, the partially unfolded OVA attached to ions, free ions, and hydrogen bonded water molecules are involved further to initiate the biomineralized crystal via self-assembly while evaporation occurs. Here the OVA fibers are formed by the unfolded OVA where the biomineralized crystals play the role of an interchain connector.

4. CONCLUSIONS

The fibrillation of OVA induced by the biomineralization of two alkali halides in the LB film of OVA was investigated. The mineral−OVA interactions were studied by pressure−area (π−A) isotherm measurement in the Langmuir monolayer. Fibrillation was monitored by the surface morphological changes of OVA−salt from globular to fibrillar aggregates by FE-SEM imaging. We observed the OVA fibrillation at the junction of the biomineralized crystals by FE-SEM imaging. In addition, HR-TEM and EDX measurements and the JCPDS data bank allowed us to identify nanostructured biomineralized crystals of salt, which are associated with this fibrillar structure. The salt-induced unfolding of protein is confirmed by a pronounced increase in β-sheet to α-helix ratio in the presence of salt by studying the FTIR spectra of the amide band in the LB film as well as by the CD spectra in solution. We suggest that ion attachment to the peptide chain leads to unfolding, and subsequent recrystallization in the transferred monolayer leads to the fibrillation of protein as well as the biomineralization of the alkali halide salts. The many body of ion−protein interactions at the high salt concentration, described in the modified DLVO theory, is responsible for the unfolding, aggregation, and finally the fibrillation of OVA. The overall findings demonstrate the fibrillation of OVA induced by the biomineralization of alkali halides as a pathway, and thus the study could have potential in the biology of amyloid formation as well as in biotechnology and materials science.

■ ASSOCIATED CONTENT

Supporting Information. HR-TEM data of biomineralized KCl crystal. This material is available free of charge via the Internet at http://pubs.acs.org.

■ AUTHOR INFORMATION

Corresponding Author

*Tel: +91-33-24734971. Fax: +91-33-24732805. E-mail: spgbt@iacs.res.in.

Present Addresses

‡Department of Physics, Narajole Raj College, Narajole, Paschim Medinipur-721211, India.

§Department of Physics, Jogesh Chandra Chaudhury College, 30, Prince Anwar Shah Road, Kolkata 700 033, India.

■ ACKNOWLEDGMENT

We thank DST, Government of India (project no. SR/S2/CMP-0051/2006) for partial financial support. Mrityunjoy Mahato thanks CSIR, Government of India, for providing the CSIR-NET fellowship.

■ REFERENCES

(1) Papapostolou, D.; Smith, A. M.; Atkins, E. D. T.; Oliver, S. J.; Ryadnov, M. G.; Serpell, L. C.; Woolfson, D. N. *Proc. Natl. Acad. Sci. U.S.A.* **2007**, *104*, 10853–10858.
(2) Pellenc, D.; Berry, H.; Gallet, O. *J. Colloid Interface Sci.* **2006**, *298*, 132–144.
(3) Pandey, N. K.; Ghosh, S.; Dasgupta, S. *J. Phys. Chem. B* **2010**, *114*, 10228–10233.
(4) Thompson, L. K. *Proc. Natl. Acad. Sci. U.S.A.* **2003**, *100*, 383–385.
(5) David, Z.; Nussinov, R.; Aleḿan, C. *Phys. Biol.* **2006**, *3*, S80–S90.
(6) Shi, J.; Wang, L.; Zhang, F.; Li, H.; Lei, L.; Liu, L.; Chen, Y. *ACS Appl. Mater. Interfaces* **2010**, *2*, 1025–1030.
(7) Jeppesen, M. D.; Westh, P.; Otzen, D. E. *FEBS Lett.* **2010**, *584*, 780–784.
(8) Juarez, J.; Lopez, S. G.; Cambon, A.; Taboada, P.; Mosquera, V. *J. Phys. Chem. B* **2009**, *113*, 10521–10529.
(9) Guijarro, J. I. a.; Sunde, M.; Jones, J. A.; Campbell, I. D.; Dobson, C. M. *Proc. Natl. Acad. Sci. U.S.A.* **1998**, *95*, 4224–4228.
(10) Uversky, V. N.; Li, J.; Fink, A. L. *J. Biol. Chem.* **2001**, *276*, 44284–44296.
(11) Linse, S.; Cabaleiro-Lago, C.; Xue, W. F.; Lynch, I.; Lindman, S.; Thulin, E.; Radford, S. E.; Dawson, K. A. *Proc. Natl. Acad. Sci. U.S.A.* **2007**, *104*, 8691–8696.
(12) Kamilya, T.; Pal, P.; Talapatra, G. B. *J. Phys. Chem. B* **2007**, *111*, 1199–1205.
(13) Kamilya, T.; Pal, P.; Mahato, M.; Talapatra, G. B. *J. Nanosci. Nanotechnol.* **2009**, *9*, 2956–2964.
(14) Kamilya, T.; Pal, P.; Mahato, M.; Talapatra, G. B. *Mater. Sci. Eng., C* **2009**, *29*, 1480–1485.
(15) Kamilya, T.; Pal, P.; Talapatra, G. B. *Colloids Surf., B* **2007**, *58*, 137–144.
(16) Kamilya, T.; Pal, P.; Talapatra, G. B. *J. Colloid Interface Sci.* **2007**, *315*, 464–474.
(17) Subburaman, K.; Pernodet, N.; Kwak, S. Y.; DiMasi, E.; Ge, S.; Zaitsev, V.; Ba, X.; Yang, N. L.; Rafailovich, M. *Proc. Natl. Acad. Sci. U.S.A.* **2006**, *103*, 14672–14677.
(18) Ghosh, S.; Mukherjee, A.; Sadler, P. J.; Verma, S. *Angew. Chem., Int. Ed.* **2008**, *47*, 2217–2221.
(19) Gilbert, P. U. P. A.; Abrecht, M.; Frazer, B. H. *Rev. Mineral. Geochem.* **2005**, *59*, 157–185.
(20) Pipich, V.; Balz, M.; Wolf, S. E.; Tremel, W.; Schwahn, D. *J. Am. Chem. Soc.* **2008**, *130*, 6879–6892.
(21) Wu, L.-Z.; Ma, B.-L.; Zou, D.-W.; Tie, Z.-X.; Wang, J.; Wang, W. *J. Mol. Struct.* **2008**, *877*, 44–49.
(22) Tronin, A.; Dubrovsky, T.; Dubrovskaya, S.; Radicchi, G.; Nicolini, C. *Langmuir* **1996**, *12*, 3272–3275.
(23) Pearce, F. G.; Mackintosh, S. H.; Gerrard, J. A. *J. Agric. Food Chem.* **2006**, *55*, 318–322.
(24) Zhao, H.; He, W.; Wang, Y.; Zhang, X.; Li, Z.; Yan, S.; Zhou, W.; Wang, G. *Mater. Lett.* **2008**, *62*, 3603–3605.
(25) Wang, X.; Kong, R.; Pan, X.; Xu, H.; Xia, D.; Shan, H.; Lu, J. R. *J. Phys. Chem. B* **2009**, *113*, 8975–8982.
(26) Mahato, M.; Pal, P.; Kamilya, T.; Sarkar, R.; Talapatra, G. B. *J. Phys. Chem. B* **2010**, *114*, 495–502.
(27) Mahato, M.; Pal, P.; Kamilya, T.; Sarkar, R.; Chaudhuri, A.; Talapatra, G. B. *J. Phys. Chem. B* **2010**, *114*, 7062–7070.
(28) Sreerama, N.; Woody, R. W. *Anal. Biochem.* **2000**, *287*, 252–260.
(29) Kamilya, T.; Pal, P.; Mahato, M.; Talapatra, G. B. *J. Phys. Chem. B* **2009**, *113*, 5128–5135.
(30) Mahato, M.; Pal, P.; Kamilya, T.; Sarkar, R.; Chaudhuri, A.; Talapatra, G. B. *Phys. Chem. Chem. Phys.* **2010**, *12*, 12997–13006.
(31) Ovalbumin (OVA). Protein Data Bank (RCSB PDB ID-1OVA).
(32) Addadi, L.; Moradian, J.; Shay, E.; Maroudas, N. G.; Weiner, S. *Proc. Natl. Acad. Sci. U.S.A.* **1987**, *84*, 2732–2736.
(33) Addadi, L.; Weiner, S. *Proc. Natl. Acad. Sci. U.S.A.* **1985**, *82*, 4110–4114.
(34) Iijima, M.; Iijima, K.; Moriwaki, Y.; Kuboki, Y. *J. Cryst. Growth* **1994**, *140*, 91–99.
(35) Zhang, W.; Liao, S. S.; Cui, F. Z. *Chem. Mater.* **2003**, *15*, 3221–3226.
(36) Hsu, W. K.; Li, W. Z.; Zhu, Y. Q.; Grobert, N.; Terrones, M.; Terrones, H.; Yao, N.; Zhang, J. P.; Firth, S.; Clark, R. J. H.; Cheetham, A. K.; Hare, J. P.; Kroto, H. W.; Walton, D. R. M. *Chem. Phys. Lett.* **2000**, *317*, 77–82.
(37) Xue, Z. H.; Hu, B. B.; Dai, S. X.; Du, Z. L. *Mater. Chem. Phys.* **2010**, *123*, 278–283.
(38) Yamaguchi, K. I.; Matsumoto, T.; Kuwata, K. *Biochemistry* **2008**, *47*, 13242–13251.
(39) Batra, P. P.; Roebuck, M. A.; Uetrecht, D. *J. Protein Chem.* **1990**, *9*, 37–44.
(40) Pal, P.; Mahato, M.; Kamilya, T.; Talapatra, G. B. *Phys. Chem. Chem. Phys.* **2011**, doi 10.1039/c0cp02277b.